Analysis of Effect of Accident Tolerant Fuel with Cr-coated Zircaloy Cladding for Large Break-Loss of Coolant Accident

Jae-Ho Bae[a*], Soon-Joon Hong[a], Tae-Sun Ro[a], Beop-Dong Jeong [a], Tongkyu Park[a], and Sungkyun Zee[a]

[a]*FNC Tech. Co. Ltd., Floor 32, Heungdeok IT Valley, 13 Heungdeok 1-ro, Giheung-gu, Yongin-si, Gyeonggi-do, 16954, Korea*

[*]Corresponding author: jhbae0822@fnctech.com

1. Introduction

Accident Tolerant Fuel (ATF) is being widely developed for improved fuel performance in normal operation, anticipated operating occurrence (AOO) and accident condition. The domestic and oversea institutions, including the USA and France, are actively conducting ATF development. Korea will soon apply for a license for loading of ATF fuel rod and assembly. It is necessary to identify changes in the expected thermal-hydraulics phenomena according to ATF loading. Coated cladding is likely to cause in boiling and quenching related phenomena.

Various types of ATF have been proposed, but this study analyzed Cr (Chromium)-coated ATF. Currently, MARS-KS code is limited in the modeling of heat structure of fuel rod, where mesh and property cannot be added outside the Zr (Zircaloy) cladding when using the gap conductance model [1]. In this study, the equivalent properties [2] of Cr-coated cladding were applied to Zion plant to analyze the PCT (Peak Cladding Temperature) according to the changes in properties through LBLOCA analysis using MARS-KS 1.5 code. In addition, effect of Cr-coated ATF compared to other sensitivity parameters.

2. Calculation of Equivalent Property

2.1 Thermal Conductivity

The Cr-coated cladding consists of UO_2 pellet, gap, zircaloy cladding, and Cr coating as shown in Fig. 1. Equivalent property is obtained by preserving the temperature of both side of the Cr-coated cladding using heat diffusion equation as follows:

$$\ddot{q} + \frac{1}{r}\frac{d}{dr}\left(kr\frac{dT}{dr}\right) = 0. \tag{1}$$

Zr cladding region (From r_1 to r_2)
    Boundary conditions are
$$T(r_2) = T_2, T(r_1) = T_1. \tag{2}$$
And the solution is
$$T(r) = \frac{T_2 - T_1}{ln(r_2/r_1)} ln\left(\frac{r}{r_2}\right) + T_2. \tag{3}$$
And, heat transfer of cladding in steady state is equal to heat generated from fuel. The heat flow is
$$\dot{q}|_{r=r_2} = -k_{12}A_2 \left[\frac{dT}{dr}\right]_{r=r_2} = q_{fuel}. \tag{4}$$

Therefore, the temperature difference between inside and outside of cladding as follows:
$$T_1 - T_2 = q_{fuel}\frac{ln(r_2/r_1)}{k_{12}2\pi L}, \tag{5}$$

where k_{12} is thermal conductivity of Zr cladding and q_{fuel} is power of fuel rod.

Cr-coating region (From r_2 to r_3)
    Boundary conditions are
$$T(r_3) = T_3, T(r_2) = T_2. \tag{6}$$
And the solution is
$$T(r) = \frac{T_3 - T_2}{ln(r_3/r_2)} ln\left(\frac{r}{r_3}\right) + T_3. \tag{7}$$
And, heat transfer of Cr-coating in steady state is equal to heat generated from fuel. Therefore, the heat flow is
$$\dot{q}|_{r=r_3} = -k_{23}A_3 \left[\frac{dT}{dr}\right]_{r=r_3} = q_{fuel}. \tag{8}$$
Thus, the temperature difference between inside and outside of Cr-coating as follows:
$$T_2 - T_3 = q_{fuel}\frac{ln(r_3/r_2)}{k_{23}2\pi L}, \tag{9}$$

where k_{23} is thermal conductivity of Cr-coating.
The summation of all temperature differences of Eq. (5) and (6) is as follows:
$$T_1 - T_3 = \frac{q_{fuel}}{2\pi L}\left[\frac{ln(r_2/r_1)}{k_{12}} + \frac{ln(r_3/r_2)}{k_{23}}\right]. \tag{10}$$
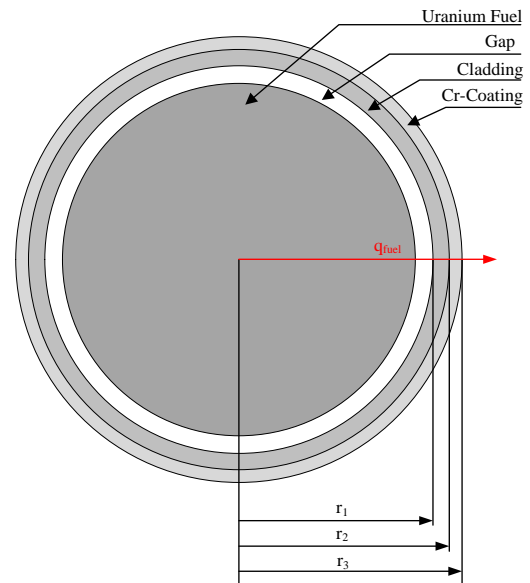

Fig. 1. Composition of Cr-coated cladding

Equivalent Cr-coated cladding (From r_1 to r_3)

Assuming that the Zr cladding and Cr-coating are one equivalent cladding, the temperature difference between the inside and outside of equivalent Cr-coated cladding can be obtained as follows. Boundary conditions and the solution are

$$T(r_3) = T_3, T(r_1) = T_1, \tag{11}$$

$$T(r) = \frac{T_3 - T_1}{\ln(r_3/r_1)} \ln\left(\frac{r}{r_3}\right) + T_3. \tag{12}$$

So the temperature difference between inside and outside of equivalent Cr-coated cladding as follows:

$$T_1 - T_3 = q_{fuel} \frac{\ln(r_3/r_1)}{k_{eq} 2\pi L}, \tag{13}$$

where k_{eq} is equivalent thermal conductivity.

In conclusion, equivalent thermal conductivity in accordance with Eq. (10) and (13) is as follows:

$$\frac{1}{k_{eq}} = \frac{1}{\ln(r_3/r_1)}\left[\frac{\ln(r_2/r_1)}{k_{12}} + \frac{\ln(r_3/r_2)}{k_{23}}\right]. \tag{14}$$

In this study, equivalent thermal conductivity were calculated assuming 10, 20, 30 μm thickness of Cr-coating on the surface of the Zr cladding. Fig. 2 shows the results of the calculated thermal conductivity. The conductivity for Zr is presented by OECD-BEMUSE Phase IV report [3]. And the Cr of that is obtained in INL report [4]. The thermal conductivity of Cr is about four times greater than that of Zr. Thus, the thermal conductivity of Cr-coated cladding is increased compared to the Zr cladding.
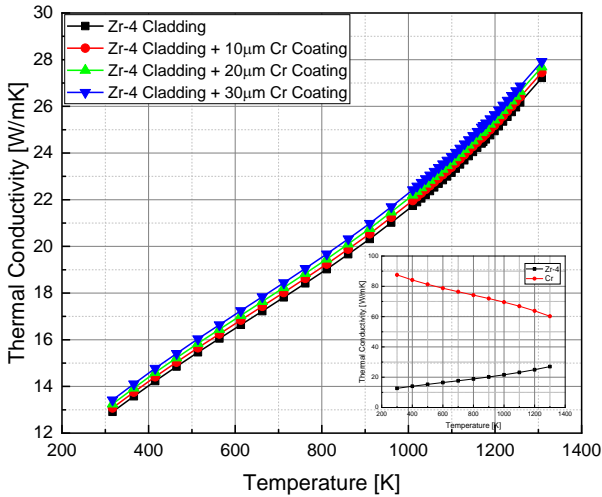

Fig. 2. Equivalent thermal conductivity

2.2 Heat Capacity

The heat capacity is related to the temperature rise of the heat structure [2]. Therefore, the equivalent heat capacity can be calculated according to the volume ratio of the Zr cladding and Cr coating as follows:

$$(\rho C_p V)_{eq} \Delta T = \sum_i (\rho C_p V)_i \Delta T, \tag{15}$$

where ρ, C_p, V, and ΔT are density, specific heat, volume, and temperature rise. Therefore, equivalent heat capacity of Zr and Cr is as follows:

$$(\rho C_p)_{eq} = \frac{V_{zr}(\rho C_p)_{zr} + V_{cr}(\rho C_p)_{cr}}{V_{zr} + V_{cr}}. \tag{16}$$

Fig. 3 shows the results of the equivalent heat capacity. The OECD-BEMUSE Phase IV report [3] provided the heat capacity of Zr for Zion plant. In addition, the heat capacity of Cr is calculated using the specific heat data of INL [4] and the density presented by Gurgen [5]. The heat capacity is shown to have larger heat capacity in the Cr-coated cladding overall, except for the part where Zr heat capacity is greater than that of Zr in the section of Zr phase change.
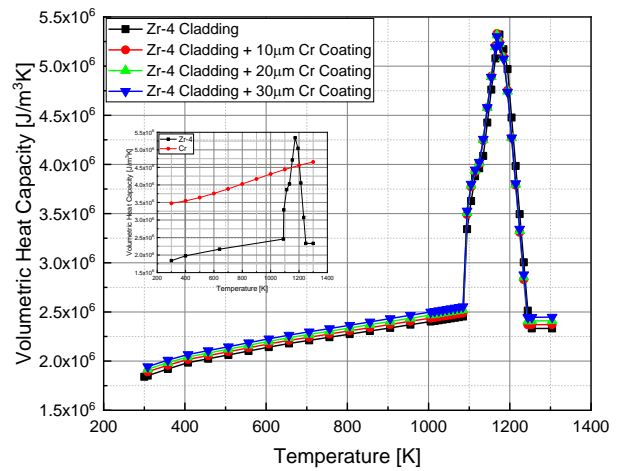

Fig. 3. Equivalent heat capacity

3. LBLOCA Analysis of Zion Plant

3.1 Zion Plant

In this study, ATF characteristics were applied for Zion plant. The Zion plant is a pressurized water reactor operated by Common-wealth Edison in the United Satates and is now permanently shut down. The core power is 3250 MWth and is WH (Westing-House) type-4 loop reactor. The MARS-KS nodalization of the Zion plant is shown in Fig. 4. The break is simulated with double-ended guillotine break. The safety injection system is composed of the accumulator and LPIS (Low Pressure Injection system) and is actuated according to trip set point. Table I presents the steady-state result. The results are similar to the reference presented by the OECD-BEMUSE Phase IV [3].
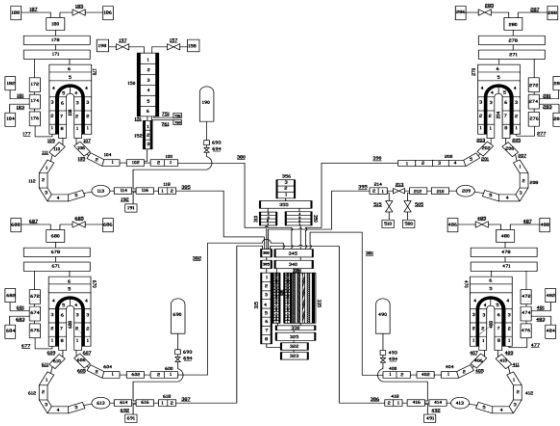
Fig. 4. MARS-KS nodalization for Zion plant [3]

Table I: Steady-state result

Plant Parameter	Target	MARS-KS
Core power [MW]	3,250.0	3,250.0
Pressure in cold leg (MPa)	15.8	15.8
Pressure in hot leg (MPa)	15.5	15.5
Pressurizer level (m)	8.8	8.8
Core outlet temperature (K)	603.0	602.6
Primary coolant flow (kg/s)	17357.0	17428.8
Secondary pressure (MPa)	6.7	6.7
SG downcomer level (m)	12.2	12.0
Feed water flow per loop (kg/s)	439.0	439.2
Accumulator pressure (MPa)	4.14	4.14
Accumulator gas volume (m^3)	15.1	15.1
Accumulator liquid volume (m^3)	23.8	23.8
RCP velocity (rad/s)	120.06	120.06

3.2 Modeling for Cr-coated Cladding

The Cr-coated cladding is modeled by calculating and applying the equivalent properties of zircaloy and chromium. The coated cladding have different diameter of the fuel rod compared to Zr cladding. Therefore, changes in variables other than equivalent properties should also be considered in MARS-KS modeling. The Cr-coated cladding is modeled in consideration of the following:

Heat structure
- Properties of cladding (thermal conductivity/heat capacity): Zr properties are replaced by the equivalent properties of Zr and Cr.
- Radius of cladding: The radius of the cladding is increased by thickness of Cr coating.

Hydraulic component
- Hydraulic volume of core: Volume is decreased by increasing the diameter of fuel rod due to Cr coating.

- Flow area of core: Flow area is decreased by increasing the total diameter of fuel rod due to Cr coating.
- Hydraulic diameter of core: Hydraulic diameter is decreased by increasing the total diameter of fuel rod due to Cr coating.

In consideration of the above, Cr-coated cladding is simulated at the Zion plant. The effect of equivalent properties and hydraulic variables on LBLOCA PCT is evaluated for three Cr-coating thickness (10, 20, 30 µm) in Zion plant.

3.3 Analysis Results

Fig. 5 and Fig. 6 show the PCT when Cr-coated cladding is applied. Table II also summarizes the calculation results of PCT in the blowdown and reflood phase. In the blowdown phase, the blowdown peak is shown to be calculated lower in all cases of coated cladding than Zr cladding. This is judged to be due to the higher equivalent thermal conductivity of coated cladding than Zr cladding, which results in faster release of fuel energy in early phase of LOCA. Reflood peak is calculated higher compared to Zr cladding when applying Cr-coated cladding. In the reflood phase, the effects of other thermal-hydraulic variables are significant, and it is not possible to accurately determine whether the effects are due to coated cladding. It is also that the quenching time is further delayed compared to the Zr cladding.
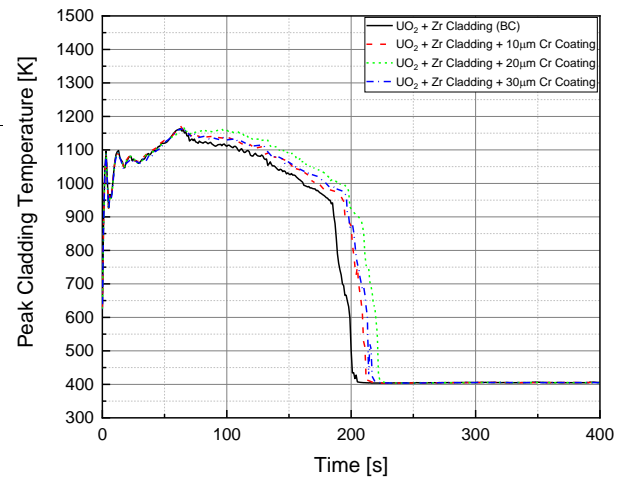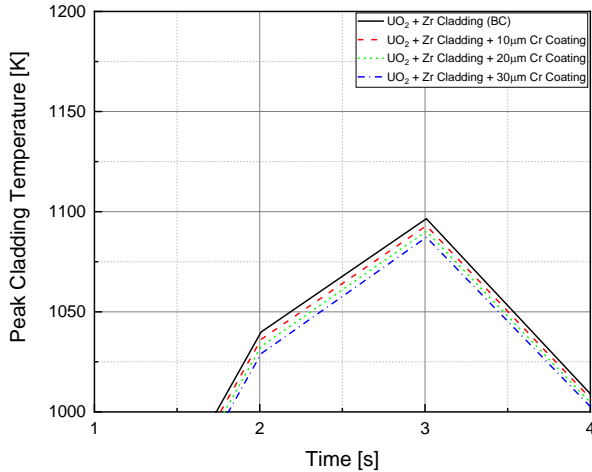

Fig. 5. Results of PCT of Cr-coated cladding

Fig. 6. Results of PCT of Cr-coated cladding (blowdown)

Table II: Comparison of PCT

	Zr-4	Zr-4+ 10μm Cr	Zr-4+ 20μm Cr	Zr-4+ 30μm Cr
Phase	PCT [K]			
Blowdown peak	1096.5	1093.0	1090.2	1087.2
Reflood peak	1163.4	1171.2	1169.6	1165.4

3.4 Relative Comparison of Cr-coated Cladding Effect

It is confirmed through LBLOCA analysis of Zion plant prior to PCT change compared to Zr cladding when Cr-coated cladding is applied. It is necessary to conduct relative comparison of how much difference caused by change in properties affects PCT relative to other sensitivity parameters. The sensitivity analysis is performed with reference to the sensitivity parameters and ranges of Zion plant LBLOCA analysis presented in OECD-BESUME phase IV (Table III) [3].

Fig. 7 compares the PCT results of the Cr-coated cladding with the results for sensitivity parameters. In contrast to most sensitivity parameter effects, it is shown that effect of Cr-coated is less than the others. Although there are PCT results of the Cr-coated cladding within the range of sensitivity parameters, the results are comparable to the effects of the sensitivity parameters in some case. Thus it is evaluated that the effect on PCT due to Cr-coated cladding is not negligible and the Cr coating should be modeled in safety analysis.

Table III: Sensitivity parameter of Zion LBLOCA analysis

| No.	Parameter	Range	
		Min	Max
1	Fuel conductivity	$value_{BC}$ − 0.4 W/mK	$value_{BC}$ + 0.4 W/mK
2	Gap conductivity	$value_{BC} \times 0.8$	$value_{BC} \times 1.2$
3	Power after scram	$value_{BC}$ − 8%	$value_{BC}$ + 8%
4	Power before scram	$value_{BC}$ − 3.3%	$value_{BC}$ + 3.3%
5	Hot rod power	$value_{BC}$ − 7.6%	$value_{BC}$ + 7.6%
6	LPIS delay (3/3)	-	$value_{BC}$ + 30 sec
7	Accumulator liquid volume (3/3)	$value_{BC}$ − 33 ft^3	$value_{BC}$ + 33 ft^3
8	Accumulator pressure (3/3)	$value_{BC}$ − 100 psig	$value_{BC}$ + 100 psig
9	Containment pressure	see Ref. [3]	
10	Hot/cold conditions for pellet radius	see Ref. [3]	
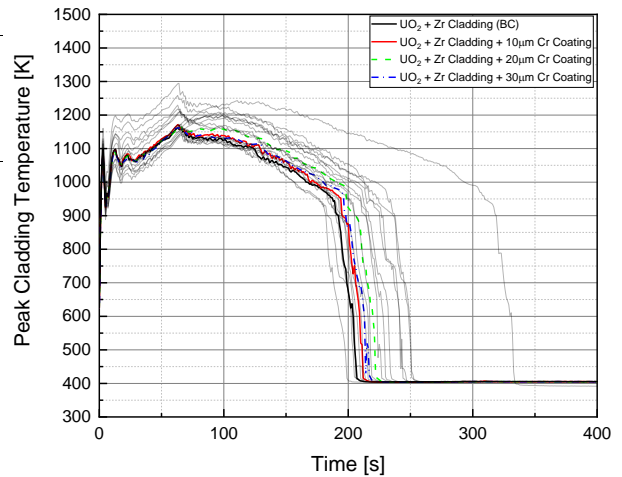
Fig. 7. Comparison of sensitivity result with Cr-coated cladding

4. Conclusions

A realistic Cr-coated cladding modeling method for MARS-KS code is currently unavailable, so the method for modeling using equivalent properties of zircaloy and chromium is used. The calculation result of equivalent properties shows slight increase in both properties in Cr-coated cladding relative to zircaloy in thermal conductivity and heat capacity. The equivalent properties are applied to LBLOCA analysis of Zion plant, and the effect of the change in properties on PCT is analyzed. The PCT is calculated low when coated cladding is applied in blowdown peak. In reflood phase, the effect on PCT could not be accurately analyzed due to non-linear effects by complex phenomena. In addition, this study conducts relative comparison with sensitivity parameters for showing the effect by Cr

coating. The calculation results show that effect of Cr coating is not negligible and should be modeled in safety analysis.

ACKNOWLEDGEMENT

REFERENCES

[1] 한국원자력안전기술원, MARS-KS code manual, 한국원자력안전기술원, KINS/RR-1822, 2018.

[2] Lee, J. et al., Design of electric core simulator system (ECSS) for large-scale integral effect test facility, Annals of Nuclear Energy 133, pp. 762-776, 2019.

[3] NEA, BESUME Phase IV Report: Simulation of a LB-LOCA in ZION Nuclear Power Plant Appendices A to D, NUCLEAR ENERGY AGENCY COMMITTEE ON THE SAFETY OF NUCLEAR INSTALLATIONS, NEA/CSNIR(2008)6/VOL2, 2008.

[4] Waigh, M. et al., Fuel Performance of Chromium-Coated Zirconium Alloy and Silicon Carbide Accident Tolerant Fuel Claddings, Idaho National Laboratory, INL-JOU-18-50119-Revison-0, 2018

[5] Gurgen, A. et al., Estimation of coping time in pressurized water reactors for near term accident tolerant fuel claddings, Nuclear Engineering and Design, Vol. 337, pp. 38-50, 2018